

# EFFECT FROM DOPING OF QUANTUM WELLS ON ENHANCEMENT OF THE MOBILITY LIMITED BY ONE-INTERFACE ROUGHNESS SCATTERING.

TRAN THI HAI

*Department of Engineering and Technology, Hong Duc University*

NGUYEN HUYEN TUNG AND NGUYEN TRUNG HONG

*Institute of Engineering Physics, Hanoi University of Science and Technology*

**Abstract.** *We present a theoretical study of the effect from doping of quantum wells (QWs) on enhancement of the mobility limited by one-interface roughness scattering. Within the variational approach, we introduce the enhancement factor defined by the ratio of the overall mobility in symmetric two-side doped square QWs to that in the asymmetric one-side counterpart under the same doping and interface profiles. The enhancement is fixed by the sample parameters such as well width, sheet carrier density, and correlation length. So, we propose two-side doping as an efficient way to upgrade the quality of QWs. The two-interface roughness scattering is also incorporated to make comparison.*

## I. INTRODUCTION

As well known, [1] enhanced mobility of two-dimensional (2D) carriers in quantum wells (QWs) is achieved by means of modulation of the decisive factors, such as electronic structure, scattering mechanisms, and confining sources. For instance, doping is an indispensable source for carrier supply to the sample, but this is a scattering mechanism for carriers moving in the in-plane. This is also a confining source along the growth direction. Doping as a scattering mechanism was more studied than as a confining source.

The role of any scattering in the in-plane depends strongly on the carrier distribution along the quantization direction, i.e., the envelop wave function. This is, in turn, fixed by confining sources. It was indicated [2–11] that roughness-related scattering dominates transport in many heterostructures, especially thin square QWs. This is determined by the wave function near the interface. It is obvious that remote one-side (1S) doping of square QWs leads to asymmetric band bending, so to an asymmetric modulation of the wave function, making some essential changes in 2D transport. Recently, [12, 13] we have presented a first successful attempt at giving the theory of 1S doping effects on 2D transport in an analytically tractable framework. Thereby, we are able to explain the experimental data about roughness-limited mobility, showing a well width dependence deviated from the power-of-six (classic) law characteristic of the flat-band (nondoped) model. Moreover, the roughness-related scatterings are remarkably strengthened, so the mobility is degraded drastically.

We find that for roughness-related scattering from two interfaces or from the doping-side interface, the mobility in a two-side doping (2S) QW are larger than that in one-side (1S)-doped, but smaller than that in undoped counterparts. For scattering from substrate-side interface, the 2S-doped QW mobility is smaller than the 1S-doped QW one. We examine the dependence of the 2S-doped QW mobility on the well width, carrier density, and correlation length. The roughness-limited mobility of 2D-doped QWs exhibits a well-width evolution deviated from the classic law for the undoped QW. Compared to the 1S-doping case, the 2S-doped QW mobility is enhanced by a rather large factor dependent on the sample parameters.

Therefore, the aim of this paper is to present a theoretical study of the dependence of mobility and its enhancement on the well width, carrier density, and correlation length limited by one-interface roughness scattering.

## II. ONE-SIDE AND TWO-SIDE DOPED SQUARE QW

To start with, we examine the effect from doping-induced band bending on the carrier distribution along the growth direction. For high enough barriers, we may take an asymmetric ( $\zeta_A(z)$ ) and symmetric ( $\zeta_S(z)$ ) envelop wave function for carriers (electrons or heavy holes) in the lowest subband of the QW as follows:

One-side doping (A):

$$\zeta_A(z) = \begin{cases} B_1 \sqrt{\pi/L} \cos(\pi z/L) e^{-c_1 z/L}, & \text{for } |z| \leq L/2 \\ 0, & \text{for } |z| > L/2 \end{cases} \quad (1)$$

Two-side doping (S):

$$\zeta_S(z) = \begin{cases} 2B_2 \sqrt{\pi/L} \cos(\pi z/L) \cosh(c_2 z/L), & \text{for } |z| \leq L/2 \\ 0, & \text{for } |z| > L/2 \end{cases} \quad (2)$$

with  $L$  as the well width. Here,  $B_1$ ,  $B_2$  and  $c_1$ ,  $c_2$  are variational parameters to be determined.

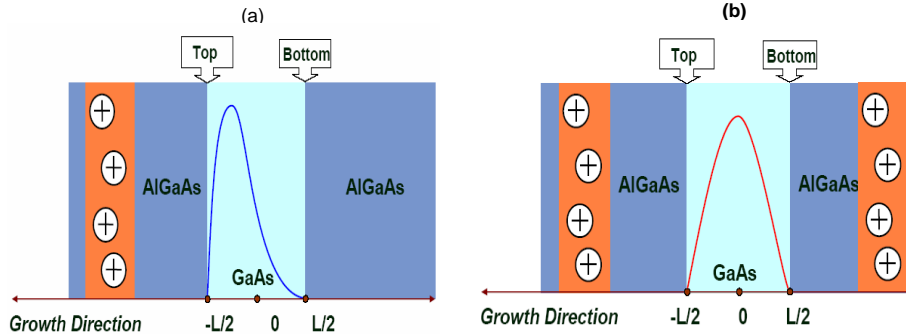


**Fig. 1.** Model for single-side and double-side doped square QWs

### III. LOW-TEMPERATURE MOBILITY

The mobility of a two-dimensional hole gas (2DHG) in  $p$ -channel QWs is one of the most important parameters fixing its performance, however, limited by various scatterings. Within the linear transport theory, the mobility at very low temperatures are determined by the transport lifetime:  $\mu = e\tau/m^*$ , with  $m^*$  as the in-plane effective mass of the carrier. The transport lifetime is represented in terms of the autocorrelation function (ACF) for each disorder by [15]:

$$\frac{1}{\tau} = \frac{1}{(2\pi)^2 \hbar E_F} \int_0^{2k_F} dq \int_0^{2\pi} d\varphi \frac{q^2}{(4k_F^2 - q^2)^{1/2}} \frac{\langle |U(\mathbf{q})|^2 \rangle}{\varepsilon^2(q)}, \quad (3)$$

Here  $\mathbf{q} = (q, \varphi)$  is the 2D momentum transfer due to a scattering event in the  $x$ - $y$  plane (in polar coordinates):  $q = |\mathbf{q}| = 2k_F \sin(\vartheta/2)$  with  $\vartheta$  as a scattering angle. The Fermi energy is given by  $E_F = \hbar^2 k_F^2 / 2m^*$ , with  $k_F = \sqrt{2\pi p_s}$  as the Fermi wave number and  $p_s$  is the sheet density. The ACF in Eq. (3),  $\langle |U(\mathbf{q})|^2 \rangle$ , is defined by an ensemble average of the 2D Fourier transform of the (unscreened) scattering potential weighted with an envelop wave function. The carriers are expected to be subject to the following scattering mechanisms: (i) surface roughness (SR), and (ii) misfit deformation potential (DP). The overall lifetime  $\tau_{\text{tot}}$  is then determined by the ones for individual disorders according to the Matthiessen rule,

$$\frac{1}{\tau_{\text{tot}}} = \frac{1}{\tau_{\text{SR}}^{(t)}} + \frac{1}{\tau_{\text{SR}}^{(b)}} + \frac{1}{\tau_{\text{DP}}^t} + \frac{1}{\tau_{\text{DP}}^b}, \quad (4)$$

where the superindices  $(t)$  and  $(b)$  refer to the top and bottom interfaces, respectively. According to Eq. (3) we ought to specify the autocorrelation function in wave-vector space  $\langle |U(\mathbf{q})|^2 \rangle$  for these scattering sources.

#### III.1. Surface roughness (SR)

First, we are dealing with scattering of the 2DHG from a rough potential barrier. The scattering potential is due to roughness-induced fluctuations in the position of the barrier [16]. The autocorrelation function for surface roughness scattering in a square QW of an arbitrary depth was derived in Ref. [17]. The result reads as follows:

$$\langle |U_{\text{SR}}^{(t/b)}(\mathbf{q})|^2 \rangle \sim (V_0 |\zeta_{A(S), \mp}|^2)^2. \quad (5)$$

where  $\zeta_{\mp} = \zeta(z = \mp L/2)$

#### III.2. Misfit deformation potential (DP)

Next, interface roughness was shown [17, 18] to produce fluctuations in a strain field in a lattice-mismatched heterostructure. These in turn act as a scattering source on charge carriers. Further, it was proved [19–21] that the misfit deformation potentials for two kinds of carrier are quite different, viz., the one for electrons is fixed by a single normal diagonal component of the strain field, whereas the one for holes by all its components. We supply the 2D Fourier transform of the misfit DP for cubic crystals. The scattering potential associated with the top interface ( $z = -L/2$ ) is given as follows for electrons: [22]. We

may obtain the ACFs for misfit DP scattering for holes in the following form:

$$\begin{aligned} \langle |U_{\text{DP}}^{(t/b)}(\mathbf{q})|^2 \rangle &= \left( \frac{\pi^{3/2} \alpha \epsilon_{\parallel} \Xi \Delta_{t/b} \Lambda_{t/b} B^2}{4L} \right)^2 \times t^2 e^{-t} [\gamma_1(c+t/2) \\ &+ \gamma_1(c-t/2) + 2\gamma_1(t/2)]^2 \frac{1}{(1 + \lambda^2 t^2 / 4n)^{n+1}} \times \left\{ \frac{3}{2} [b_s(K+1)]^2 \right. \\ &\left. (1 + \sin^4 \varphi + \cos^4 \varphi) + \left( \frac{d_s G}{4c_{44}} \right)^2 (1 + \sin^2 \varphi \cos^2 \varphi) \right\}. \end{aligned} \quad (6)$$

in the well ( $|z| \leq L/2$ ) and zero elsewhere. In Eq. (6)  $b_s$  and  $d_s$  are the shear deformation potential constants of the well layer, and  $\epsilon_{\parallel}$  is the lattice mismatch specified by the Ge content and the widths of the well and barrier, and its anisotropy ratio is yielded by

$$\alpha = 2 \frac{c_{44}}{c_{11} - c_{12}}, \quad (7)$$

its elastic constants by

$$K = 2 \frac{c_{12}}{c_{11}}, \quad G = 2(c_{11} + 2c_{12}) \left( 1 - \frac{c_{12}}{c_{11}} \right), \quad (8)$$

with  $c_{ij}$  as its elastic stiffness constants. It is clearly seen from Eq. (6) that the deformation potential related to a rough interface decays rapidly (exponentially) with an increase of the distance measured therefrom.

### III.3. Mobility enhancement

We now consider the case that roughness-related scatterings (SR and misfit DP) dominate the low-temperature transport in remote-doped square QWs. As a measure of the advantage of the symmetric modulation of the square QW over its asymmetric modulation, we introduce an enhancement factor. This is defined by the ratio of the overall mobility in the 2S-doped QW ( $\mu_{\text{tot}}^{\text{s,BT}}$ ) to that in the 1S-doped counterpart ( $\mu^{\text{a,BT}}$ ) with the same sheet carrier density and the same interface profile,

$$Q_{BT}(L, p_s; \Lambda) = \frac{\mu_{\text{tot}}^{\text{s,BT}}(L, p_s; \Delta, \Lambda)}{\mu_{\text{tot}}^{\text{a,BT}}(L, p_s; \Delta, \Lambda)}. \quad (9)$$

Since the roughness amplitude drops out of the ratio, this depends on the well width, sheet carrier density, and correlation length as shown explicitly. Further, this is shaped by the features of the QW structure.

(i) bottom-interface scattering ( $Q_B$ ):

$$Q_B(L, p_s; \Lambda) = \frac{\mu_{\text{tot}}^{\text{s,B}}(L, p_s; \Delta_b, \Lambda_b)}{\mu_{\text{tot}}^{\text{a,B}}(L, p_s; \Delta_b, \Lambda_b)}. \quad (10)$$

(ii) top-interface scattering ( $Q_T$ ):

$$Q_T(L, p_s; \Lambda) = \frac{\mu_{\text{tot}}^{\text{s,T}}(L, p_s; \Delta_t, \Lambda_t)}{\mu_{\text{tot}}^{\text{a,T}}(L, p_s; \Delta_t, \Lambda_t)}. \quad (11)$$

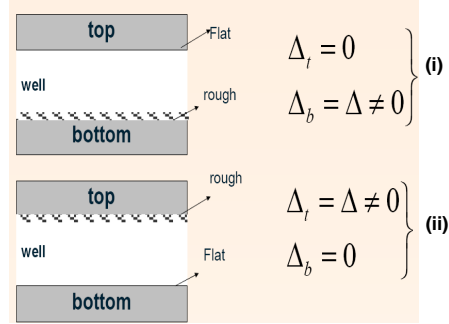


**Fig. 2.** We introduce the enhancement factor for the cases of 1-interface scattering, such as (i) bottom-interface scattering ( $Q_B$ ): the bottom (substrate-side) interface is rough, while the top (doping-side) one is flat ( $\Delta_t = 0$ ), and (ii) top-interface scattering ( $Q_T$ ): the top interface is rough, while the bottom one is flat ( $\Delta_b = 0$ ).

#### IV. NUMERICAL RESULTS AND CONCLUSION

In this section, we apply theory [12–14] in order to understand the properties of low-temperature transport in remote doped square QWs. We next examine the above functional dependence of the enhancement factor  $Q$  for the normal case, where the two QW interfaces are described by the same roughness profile.

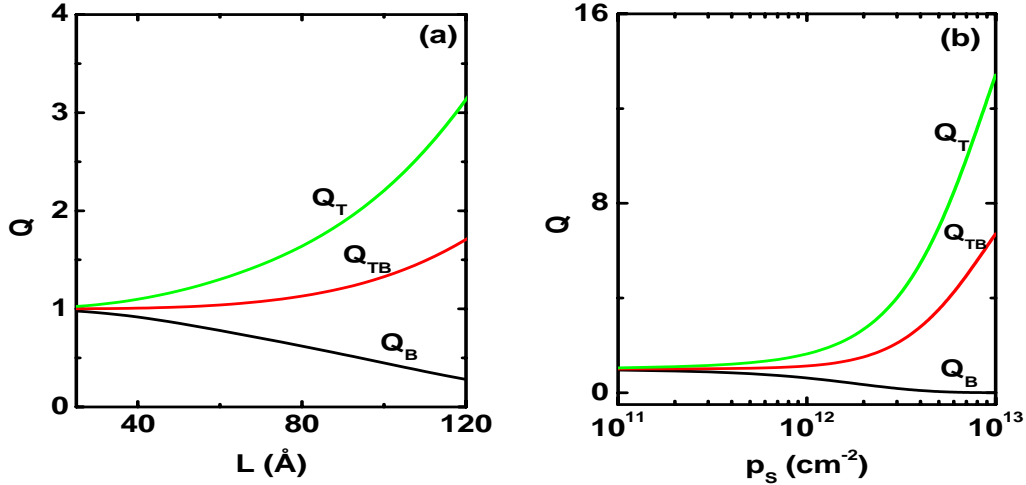


**Fig. 3.** Mobility enhancement factor  $Q$  for the p-type square QW with a correlation length  $\Lambda = 10 \text{ \AA}$  vs the well width  $L$  for a sheet hole density  $p_s = 10^{12} \text{ cm}^{-2}$  (a) and  $Q$  vs the sheet hole density with a correlation length  $\Lambda = 10 \text{ \AA}$  and a well width  $L = 80 \text{ \AA}$  (b).

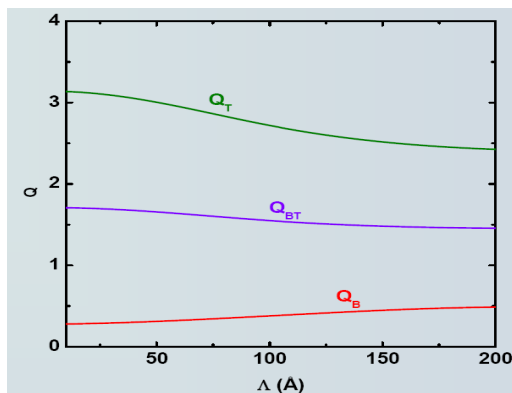


**Fig. 4.** Mobility enhancement factor  $Q$  for the p-type square QW vs the correlation length  $\Lambda$  for a well width  $L = 120 \text{ \AA}$  and a sheet hole density  $p_s = 10^{12} \text{ cm}^{-2}$ .

(i) It follows from Fig. 3 that the enhancement factor may be increased when raising the well width and carrier density in some region. For instance, at a small carrier density, the factor is nearly equal to unity:  $Q \sim 1$  for  $p_s = 10^{11} \text{ cm}^{-2}$ . However, at its large values, this is high, for instance, as seen from Fig.3:  $Q = 7.24$  for  $p_s = 10^{13} \text{ cm}^{-2}$ ,  $L = 110 \text{ \AA}$ , and  $\Lambda = 10 \text{ \AA}$ .

(ii) Figures 3, 4 reveal that the mobility enhancement is larger for top-interface, but smaller for bottom-interface scattering:  $Q_t > Q > 1$ , and  $Q_b < 1$ . Thus, 2S doping is of advantage in case of 2-interface and top-interface scatterings, while of disadvantage in case of bottom-interface one. This is in accordance with asymmetric modification of the envelop function induced by 1S doping of square QWs, namely, the electron distribution is shifted towards the doping-side interface, so that the roughness-related scattering from the top-interface is stronger, but from the bottom-interface the weaker.

(iii) As usual, we evaluated a two-interface scattering and showed the modification for one-interface scattering. For 1S-doped and 2S-doped QWs under one-interface scattering, we calculated the mobility enhancement for top- and bottom-interface scatterings and compared them with the two-interface counterpart. As clearly observed from Fig.3,.4 the factor  $Q$  for top-interface is almost the largest due to the band-bending effect.

(iv) We hope that our analytic results stimulate theoretical investigations and help to clarify future experimental results.

## REFERENCES

- [1] T. Ando, A. B. Fowler, and F. Stern, *Rev. Mod. Phys.* **54** (1982) 437.
- [2] Y. H. Xie, D. Monroe, E. A. Fitzgerald, P. J. Silverman, F. A. Thiel, and G. P. Watson, *Appl. Phys. Lett.* **63** (1993) 2263.
- [3] K. L. Campman, H. Schmidt, A. Imamoglu, and A. C. Gossard, *Appl. Phys. Lett.* **69** (1996) 2554.
- [4] H. Çelik, M. Cankurtaran, A. Bayrakli, E. Tiras, and N. Balkan, *Semicon. Sci. Technol.* **12** (1997) 389.
- [5] N. Balkan, R. Gupta, M. Cankurtaran, H. Çelik, A. Bayrakli, E. Tiras, and M. Ç. Arıkan, *Superlattices Microstruct.* **22** (1997) 263.

- [6] M. Cankurtaran, H. Çelik, E. Tiras, A. Bayrakli, and N. Balkan, *Phys. Status Solidi* **B207** (1998) 139.
- [7] C. Gerl, S. Schmult, H.-P. Tranitz, C. Mitzkus, and W. Wegscheider, *Appl. Phys. Lett.* **86** (2005) 252105.
- [8] C. Gerl, S. Schmult, U. Wurstbauer, H.-P. Tranitz, C. Mizkus, and W. Wegscheider, *Physica* **E32** (2006) 258.
- [9] B. Rössner, H. von Känel, D. Chrastina, G. Isella, and B. Batlogg, *Thin Solid Films* **508** (2006) 351.
- [10] M. Myronov, K. Sawano, and Y. Shiraki, *Appl. Phys. Lett.* **88** (2006) 252115.
- [11] F. Szmulowicz, S. Elhamri, H. J. Haugan, G. J. Brown, and W. C. Mitchel, *J. Appl. Phys.* **101** (2007) 04706.
- [12] D. N. Quang and N. H. Tung, *Phys. Rev.* **B77** (2008) 125335.
- [13] D. N. Quang, N. H. Tung, D. T. Hien, and T. T. Hai, *J. Appl. Phys.* **104** (2008) 113711.
- [14] D. N. Quang, N. H. Tung, N. T. Hong, and T. T. Hai, *Comm. in Phys.* **20** (2010) 193.
- [15] A. Gold, *Phys. Rev.* **B35** (1987) 723; **38** (1988) 10798.
- [16] T. Ando, A. B. Fowler, and F. Stern, *Rev. Mod. Phys.* **54** (1982) 437.
- [17] D. N. Quang, V. N. Tuoc, and T. D. Huan, *Phys. Rev.* **B68** (2003) 195316
- [18] R. M. Feenstra and M. A. Lutz, *J. Appl. Phys.* **78** (1995) 6091.
- [19] D. N. Quang, V. N. Tuoc, T. D. Huan, and P. N. Phong, *Phys. Rev.* **70B** (2004) 195336.
- [20] G. L. Bir and G. E. Pikus, *Symmetry and Strain Induced Effects in Semiconductors* (Wiley, New York, 1974).
- [21] C. G. Van de Walle, *Phys. Rev.* **B39** (1989) 1871.
- [22] D. N. Quang, V. N. Tuoc, N. H. Tung, and T. D. Huan, *Phys. Rev. Lett.* **89** (2002) 077601; *Phys. Rev.* **68B** (2003) 153306.

*Received 15 September 2010.*